

Published in final edited form as:

*Toxicol Lett.* 2013 April 26; 218(3): 299–307. doi:10.1016/j.toxlet.2012.12.024.

## Manganese-Induced Oxidative DNA Damage in Neuronal SH-SY5Y Cells: Attenuation of thymine base lesions by glutathione and N-acetylcysteine

Adrienne P. Stephenson<sup>1,\*</sup>, Jeffrey A. Schneider<sup>2,\*</sup>, Bryant C. Nelson<sup>2,\*</sup>, Donald H. Atha<sup>2,\*</sup>, Ashok Jain<sup>1</sup>, Karam F. A. Soliman<sup>1</sup>, Michael Aschner<sup>3</sup>, Elizabeth Mazzio<sup>1</sup>, and R. Renee Reams<sup>1,#</sup>

Adrienne P. Stephenson: lapier@hotmail.com; Jeffrey A. Schneider: jschneid90@gmail.com; Bryant C. Nelson: bryant.nelson@nist.gov; Donald H. Atha: donald.atha@nist.gov; Ashok Jain: ashok.jain@asurams.edu; Karam F. A. Soliman: karam.soliman@fam.u.edu; Michael Aschner: michael.aschner@vanderbilt.edu; Elizabeth Mazzio: Elizabeth.Mazzio@fam.u.edu; R. Renee Reams: renee.reams@fam.u.edu

<sup>1</sup>College of Pharmacy & Pharmaceutical Sciences, Florida A&M University, Tallahassee, Florida 32307 USA

<sup>2</sup>Biosystems and Biomaterials Division, National Institute of Standards and Technology, Gaithersburg, MD 20899 USA

<sup>3</sup>Department of Pediatrics, Vanderbilt University Medical Center, TN, 37232 USA

### Abstract

Manganese (Mn) is an essential trace element required for normal function and development. However, exposure to this metal at elevated levels may cause manganism, a progressive neurodegenerative disorder with neurological symptoms similar to idiopathic Parkinson's disease (IPD). Elevated body burdens of Mn from exposure to parental nutrition, vapors in mines and smelters and welding fumes have been associated with neurological health concerns. The underlying mechanism of Mn neurotoxicity remains unclear. Accordingly, the present study was designed to investigate the toxic effects of Mn<sup>2+</sup> in human neuroblastoma SH-SY5Y cells. Mn<sup>2+</sup> caused a concentration dependent decrease in SH-SY5Y cellular viability compared to controls. The LD<sub>50</sub> value was 12.98 μM Mn<sup>2+</sup> (p < 0.001 for control vs. 24h Mn treatment). Both TUNEL and annexin V/propidium iodide apoptosis assays confirmed the induction of apoptosis in the cells following exposure to Mn<sup>2+</sup> (2 μM, 62 μM or 125 μM). In addition, Mn<sup>2+</sup> induced both the formation and accumulation of DNA single strand breaks (via alkaline comet assay analysis) and oxidatively modified thymine bases (via gas chromatography/mass spectrometry analysis). Pre-incubation of the cells with characteristic antioxidants, either 1 mM N-acetylcysteine or 1 mM glutathione reduced the level of DNA strand breaks and the formation of thymine base lesions,

© 2013 Elsevier Ireland Ltd. All rights reserved.

#Corresponding Author: R. Renee Reams, Room 127 Dyson Bldg, 1520 Martin Luther King Blvd, College of Pharmacy & Pharmaceutical Sciences, Florida A&M University, Tallahassee, Florida 32307, USA, Ph#: 850-561-2672, Facsimile #: 850-599-3171, Renee.reams@fam.u.edu.

\*These authors shared equally in this work

Disclaimer:

Certain commercial equipment, instruments and materials are identified in this paper to specify an experimental procedure as completely as possible. In no case does the identification of particular equipment or materials imply a recommendation or endorsement by the National Institute of Standards and Technology nor does it imply that the materials, instruments, or equipment are necessarily the best available for the purpose.

**Publisher's Disclaimer:** This is a PDF file of an unedited manuscript that has been accepted for publication. As a service to our customers we are providing this early version of the manuscript. The manuscript will undergo copyediting, typesetting, and review of the resulting proof before it is published in its final citable form. Please note that during the production process errors may be discovered which could affect the content, and all legal disclaimers that apply to the journal pertain.

suggesting protection against oxidative cellular damage. Our findings indicate that 1) exposure of SH-SY5Y cells to Mn promotes both the formation and accumulation of oxidative DNA nucleotide base damage, 2) SH-SY5Y cells with accumulated DNA damage are more likely to die via an apoptotic pathway and 3) the accumulated levels of DNA damage can be abrogated by the addition of exogenous chemical antioxidants. This is the first known report of Mn<sup>2+</sup>-induction and antioxidant protection of thymine lesions in this SH-SY5Y cell line and contributes new information to the potential use of antioxidants as a therapeutic strategy for protection against Mn<sup>2+</sup>-induced oxidative DNA damage.

## Keywords

DNA damage; oxidative stress; manganese; SH-SY5Y cells; antioxidants; glutathione; N-acetylcysteine; thymine base; Mn<sup>2+</sup>

## 1. Introduction

Manganese (Mn) is an essential metal for the function of many enzymes, such as Mn-superoxide dismutase (Mn-SOD), pyruvate carboxylase, arginase and glutamine synthase (GS). In addition, Mn promotes normal growth and development and can substitute for magnesium and calcium in many enzyme-catalyzed kinase reactions (Baly et al. 1985; Brock and Walker 1980; Takeda and Avila 1986). Humans get exposed to Manganese primarily thru occupational exposures, as in the case of miners, smelters, welders and workers in battery factories and more recently, the general public may be getting more exposure to Mn via addition of Manganese to gasoline as an antiknock agent. (Bowler et al., 2007; 2011). Though an essential element in humans, exposures to high levels of Mn in occupational and environmental settings can lead to a disorder termed manganism, which is an excessive accumulation of Mn in the basal ganglia (Dorman et al. 2006). Researchers (Gorell et al. 1999a; Gorell et al. 1999b; Kim et al. 1999; Racette et al. 2001) have shown that excess brain Mn is a risk factor for IPD. Occupational exposure to Mn for >20 years or combined long-term exposures to Mn and Al (>30 years) were associated with increased prevalence of IPD (Gorell et al. 1999; Normandin et al. 2002). Mechanisms by which Mn induces neuronal damage are not well defined, its neurotoxicity appears to be regulated by a number of factors, including oxidative injury, mitochondrial dysfunction and neuroinflammation (Stredrick et al. 2004; Chen and Liao 2002; Seth et al. 2002; Weber et al. 2002; Worley et al. 2002).

Mn exists in eleven oxidation states, of these eleven, Mn<sup>2+</sup>, Mn<sup>3+</sup> are commonly found in living tissue. The Mn<sup>2+</sup> state is the most stable and is largely found inside of cells. The oxidation state and solubility of the Mn salt will govern its absorption across the GI tract, but once it is within the blood all forms of Mn (absorbed as Mn<sup>2+</sup>) will behave in an analogous way. Mn is not absorbed across the membranes as a salt, so the free Mn, based on the mass action law dictates that at all times an infinitesimal amount of free Mn<sup>2+</sup> will exist. Whatever its origin (the anion bound to it) will determine the rate of absorption and the amount, but the process will be identical. It is now understood that Mn enters cells via a number of transport mechanisms. In the +3 oxidation state (Mn<sup>3+</sup>), the evidence suggests that Mn is transported via the transferrin (Tf) receptor mechanism. Under normal conditions, the Mn arriving at the liver in the portal circulation is protein bound. Within the plasma, approximately 80% of manganese is bound to the iron-carrying protein, transferrin (Aisen et al., 1969); Critchfield and Keen, 1992). Mn uptake into a specific cell type is thus determined by the activity of each type of uptake mechanism expressed in that cell type and the oxidation state of the Mn reaching the cell. Once inside the cell, most of the Mn is found in the mitochondrial and nuclear fractions and is largely in the 2+ oxidation state. In the

present study, we chose to the Mn<sup>2+</sup> salt for the entire study because of its solubility. The salt anion has no significance on Mn<sup>2+</sup> salt toxicity. The salt (anion) will determine the rate of absorption, the less soluble the salt, the less Mn that will be taken up. However, the transport itself will remain the same irrespective of the salt, and will occur via the divalent metal transporter 1 (DMT1), a Mn citrate transporter, a stored activated Ca<sup>2+</sup> channel, the ZIP8 mechanism, and the ZIP 14 mechanism (ZIP8 (SLC39A8) and ZIP 14 are members of the ZIP family of metal-ion transporters. ZIP8 and ZIP14, which are closely related, transport iron, zinc, manganese, and cadmium. (Wang CY, et al, 2012). In the present study, SH-SY5Y cells were used as a model neuronal-like system to test the hypothesis that Mn<sup>2+</sup> induces apoptotic cell death through a series of events involving oxidatively damaged DNA. Human neuroblastoma SH-SY5Y cells, a third generation subclone of SK-SN-SH cells are a catecholaminergic neuroblastoma cell line derived from the brain (Biedler et al. 1973). Upon differentiation, SH-SY5Y cells adopt a neuronal-like phenotype and stop proliferating (Jalava et al. 1992; Pahlman et al. 1981). In this study, we exposed SH-SY5Y cells to Mn<sup>2+</sup> and evaluated the cells on the basis of cellular viability, induction of apoptosis and on the formation and accumulation of DNA single strand breaks and oxidatively-induced DNA base modification.

## 2. Materials and Methods

### 2.1. Chemicals

Manganese chloride tetrahydrate (MnCl<sub>2</sub>·4H<sub>2</sub>O), N-acetylcysteine (NAC), glutathione (GSH), *all trans* retinoic Acid (RA) and resazurin (indicator dye for cell viability, also known as Alamar Blue) were purchased from Sigma-Aldrich (St. Louis, MO). Heat-inactivated fetal bovine serum (FBS), Dulbecco's-modified Eagle's medium (DMEM)/F-12, penicillin-streptomycin, trypsin, Hanks's buffered saline solution (HBSS) and phosphate buffered-saline 1X (PBS-1X pH7.4) were purchased from Gibco (catalog number 10010-049). Annexin-V-FITC apoptosis detection kit was purchased from BD Bioscience (San Jose, CA). The Apoptag<sup>®</sup> *in situ* detection kit was obtained from Chemicon (Temecula, CA). 4', 6-diamidino-2-phenylindole (DAPI) vectashield mounting media was purchased from Vector Laboratories (Burlingame, CA). Human neuroblastoma SH-SY5Y cells (catalog # 2266) were obtained from the American Type Culture Collection (ATCC) (Manassas, VA). The DNeasy Mini kit was obtained from Qiagen, Inc. (Valencia, CA).

### 2.2. Cell culture

SH-SY5Y cells were maintained and cultured in a humidified atmosphere of 5% CO<sub>2</sub>-95% air at 37°C. SH-SY5Y cells were grown in DMEM/F12 nutrient mixture (1:1) supplemented with 10% FBS, and penicillin/streptomycin (50 IU/mL). The medium was changed every 4 to 5 days. For all experimental conditions, serum was reduced to 2% fetal bovine serum. Cells were differentiated for 7-days using 10 μM *all trans*-retinoic acid. Prior to treatment, cells were viewed under the microscope to assess differentiation. Cells were considered differentiated once 80% or more of the cells demonstrated neurite outgrowth extensions > 2 to 3 times longer than the body width of the cell.

### 2.3. Alamar Blue cell viability assay

SH-SY5Y cells were seeded at a density of 5×10<sup>4</sup> cells in 100 μL in a 96-well plate format. Cells were incubated in the presence or absence of Mn<sup>2+</sup> (0 μM to 1000 μM MnCl<sub>2</sub>) for 24 h and 48 h. (Note, hereafter in this manuscript MnCl<sub>2</sub> will be referred to as Mn<sup>2+</sup>, In addition, the symbol M is used in this manuscript in place of SI units mol/L). At the end of the respective incubation period, 25 μL of resazurin (0.5 mg/mL) prepared in HBSS was added to each well followed by incubation for 4 h to 6 h at 37°C. Viable cells convert the oxidized form of the dye (resazurin) to its reduced form (resorufin). Fluorescence was read

on a microplate fluorometer at 550/580 nm (excitation/emission) wavelengths (Cambridge Technologies, Inc.). Cell viability was expressed as percentage of the control cell cultures.

#### 2.4. DAPI/TUNEL apoptosis assay

The Apoptag *in situ* detection kit with DAPI nuclear staining was used to assess apoptosis in SH-SY5Y cells treated with Mn<sup>2+</sup> at 2  $\mu$ M, 62  $\mu$ M, and 125  $\mu$ M following the manufacturer's protocol with slight modifications. After treatment with Mn<sup>2+</sup>, cells were harvested by trypsinization and washed with PBS once. Cells were then fixed in 4% paraformaldehyde, 2% sucrose and 1% phenol, and incubated overnight at room temperature. The *in situ* labeled nuclei were observed and photographed with a fluorescence microscope (Olympus IX70-D70 system) attached to a digital camera (Olympus America/IX-SPT).

#### 2.5. Annexin V/propidium iodide flow cytometry apoptosis assay

Apoptotic and necrotic cells were quantified by annexin V binding and propidium iodide (PI) uptake following the manufacturer's instructions. SH-SY5Y cells were plated at a density of  $1 \times 10^6$  cells in 5 mL and exposed to Mn<sup>2+</sup> (2  $\mu$ M, 62  $\mu$ M and 125  $\mu$ M) for 24 h. Cells were collected by centrifugation and washed twice with 5 mL cold 1X PBS. Cells were resuspended in 1X binding buffer at a concentration of  $1 \times 10^6$  cells/ml. Approximately 100  $\mu$ L of each sample were transferred to a 5 mL conical tube. Annexin V FITC (5  $\mu$ L) and PI 5  $\mu$ L (50  $\mu$ g/mL) were added to each sample and incubated in the dark for 15 min. 1X binding buffer (400  $\mu$ L) was then added to each tube for an additional 25 min before the apoptotic level was analyzed by flow cytometry.

#### 2.6. Alkaline comet assay

The alkaline comet assay was performed as described by Singh et al., with minor modifications. Briefly, SH-SY5Y cells were incubated in the presence or absence of Mn<sup>2+</sup> (2  $\mu$ M or 62  $\mu$ M) for 24 h at 37 °C. In a separate experiment, SH-SY5Y cells were pre-treated for 3 h with the thiol-based antioxidants, (1 mM GSH or 1 mM) NAC followed by 24 h exposure to Mn<sup>2+</sup> (2  $\mu$ M and 62  $\mu$ M). Following exposure to Mn<sup>2+</sup>, cells were washed with ice-cold PBS, trypsinized and centrifuged at 1200 rpm for 5 min. Subsequently, 100  $\mu$ l cell suspension containing  $2 \times 10^4$  cells were mixed with 900  $\mu$ L 0.75% low-melting point agarose and immediately spread on frosted microscope slides pre-coated with 0.75% high-melting point agarose. The cell-gel sandwich was covered with a coverslip and incubated to allow gel solidification for 10 min at 4°C. After removal of the cover slips, the slides were immersed in ice-cold lysis solution (2.5 M NaCl, 100 mM EDTA, 10 mM Tris, 1% Triton X-100, pH 10) for 1 h at 4°C to remove cell proteins. After lysis, slides were placed in freshly prepared electrophoresis buffer (300 mM NaOH, 1 mM EDTA, pH 13) for 20 min to allow DNA unwinding before electrophoresis. Electrophoresis was performed for 30 min at 25 V (300 mA). All of the above steps were conducted under low light to prevent additional DNA damage. After electrophoresis, the slides were neutralized (0.4 M Tris, pH 7.5), washed and stained with propidium iodide (2.5  $\mu$ g/mL). After drying overnight at room temperature, gels were analyzed with a fluorescence microscope.

#### 2.7. Comet slide analysis

Images of 25 randomly selected nuclei, out of a field containing 100 cells, were analyzed for each treatment. Slides were viewed on an inverted microscope with an epifluorescence accessory (Leica-Optiphas) and images were transferred to a computer with a digital camera. Imaging was performed with the software analysis system Comet 5.5 (Kinetic Imaging, Nottingham, UK). This software defines head and tail regions and evaluates a range of derived parameters including tail moment, an index of DNA damage that considers

both the tail length (comet length), and the fraction of DNA in the comet tail ( $TM = \% \text{ DNA in tail} \times \text{tail length} / 100$ ) to evaluate the length of DNA migration.

## 2.8. Oxidatively modified DNA base damage measurements using gas chromatography/mass spectrometry (GC/MS)

Isolation of genomic DNA was carried out using a Qiagen (Qiagen.com) DNeasy mini kit. Extracted DNA pellets were washed three times with ice cold 70% ethanol and once with ice cold absolute ethanol. The DNA pellets were dried and then solubilized in distilled and deionized water (ddH<sub>2</sub>O). DNA aliquots of approximately 50 µg were prepared from each sample and stable isotope-labeled versions [FapyGua(<sup>13</sup>C<sup>15</sup>N<sub>2</sub>), 8-OH-Gua(<sup>15</sup>N<sub>5</sub>), 5-OH-5-MeHyd(<sup>13</sup>C <sup>15</sup>N<sub>2</sub>)] of each of the investigated DNA base lesions were added, the samples were dried under vacuum and then stored at 4°C prior to enzymatic digestion. During enzymatic digestion, the samples were dissolved in a buffer consisting of 50 mM sodium phosphate, 100 mM potassium chloride, 1 mM EDTA and 100 µM dithiothreitol (pH 7.4). To this solution, 1 µg of Fpg DNA glycosylase was added and the digestion was carried out at 37°C for 1 h. The digestion was terminated with the addition of ice cold ethanol and the sample was incubated at -20 °C. The samples were centrifuged at 14,000 rpm for 30 min and the supernatants containing the excised oxidized bases were then collected and the solvent was removed by vacuum desiccation. The samples were solubilized in ddH<sub>2</sub>O, lyophilized and then derivatized to trimethylsilyl esters using BSFTA/1% trimethylchlorosilane in pyridine (120°C for 30 min.). GC/MS analysis in selected ion monitoring mode was performed on the derivatized samples as described previously by Reddy et al., 2004.

## 2.9. Statistical analysis

Statistical analysis were conducted with Graph Pad Prism 3.0. All results are expressed as means with standard deviation using a minimum of 3 independent experiments each performed in triplicates. Differences between mean values and multiple groups were analyzed by one-way analysis of variance (ANOVA) with a *post-hoc* Tukey's test. Statistical significance was set at  $p < 0.05$ .

## 3. Results

### 3.1 Manganese decreased SH-SY5Y cell viability

Our working hypothesis was that manganese could induce cell death in SH-SY5Y neuronal-like cells via an apoptotic mechanism because of its oxidative properties. To begin to test this hypothesis, we studied the effect of Mn<sup>2+</sup> on SH-SY5Y cell viability. Our approach used the Alamar Blue assay to determine the effect of Mn<sup>2+</sup> on cell viability of SH-SY5Y cells at three exposure times; 24h, 48h & 72 h after treatment with 0 µM to 500 µM manganese chloride. The results (Figure 1A) show a plot of MnCl<sub>2</sub> vs. percent cell viability (y-axis) at a 24 h incubation period. Mn<sup>2+</sup> caused a statistically significant ( $p < 0.001$ ) decrease in SH-SY5Y cellular viability at concentrations as low as 2 µM compared to controls. The LD<sub>50</sub> value was 12.98 µM Mn ( $p < 0.001$  for control vs. 24 h Mn<sup>2+</sup> treatment). Figure 1B shows a differential profile of cell viability over 24h to 72 h incubation periods.

### 3.2. In situ DNA nick end label TUNEL staining for cellular apoptosis

To address whether Mn<sup>2+</sup>-induced cell death was mediated by apoptotic mechanisms we used the *in situ* DNA Nick End Labeling TUNEL assay to detect the 3'-hydroxyl end of fragmented DNA. We chose to study apoptosis at manganese concentrations ranging from 0 to 125 µM. We examined sub-lethal concentrations of manganese in order to capture early onset of apoptosis and avoid studying cells whose viability had been severely compromised. Figure 2 shows representative photomicrographs of SH-SY5Y neuronal-like cells

undergoing apoptosis following exposure to 2  $\mu\text{M}$  and 62  $\mu\text{M}$  of  $\text{Mn}^{2+}$ . Positive TUNEL staining (Figure 2, frames D–F) was observed in SH-SY5Y cells at 24 h following  $\text{Mn}^{2+}$  exposure. (Note: the selected Mn exposure concentrations arose arbitrarily as a result of serially diluting the stock Mn solution (1000  $\mu\text{M}$ ). DAPI nuclear staining overlaid with TUNEL (Figure 2, frames A–C) was utilized to identify chromatin condensation, a morphological characteristic of apoptosis. Cells that displayed nuclear condensation were also TUNEL positive. Necrosis was ruled out, indirectly; by treating the SH-SY5Y cells with staurosporine and comparing the morphological changes for SH-SY5Y cells exposed to staurosporine to the morphological changes in the presence of  $\text{Mn}^{2+}$ . The protein kinase inhibitor, staurosporine, is widely used to induce apoptosis in neuronal, neuronal-like and non-neuronal cells (Falcieri et al 1993). Added  $\text{Mn}^{2+}$  ranging from 2  $\mu\text{M}$  to 250  $\mu\text{M}$  for 24 h produced the same cell morphology as staurosporine.

### 3.3 Annexin V/propidium iodine flow cytometric assessment for cellular apoptosis

To confirm  $\text{Mn}^{2+}$  induced cellular apoptosis, the SH-SY5Y cells were independently treated with  $\text{Mn}^{2+}$  and evaluated with annexin V/PI staining and flow cytometry (Figure 3). The fraction of annexin V-positive SH-SY5Y cells was 0% before treatment and 5.64%, 5.74% and 5.41% after 24 h treatment with  $\text{Mn}^{2+}$  at 2  $\mu\text{M}$ , 62  $\mu\text{M}$  and 125  $\mu\text{M}$ , respectively. In summary, the data indicated that all of the above  $\text{Mn}^{2+}$  exposures induced early onset of apoptotic cell death, compared to the control.

### 3.4 Manganese induced DNA single strand breaks in SH-SY5Y cells

We reasoned that  $\text{Mn}^{2+}$ -induced apoptosis may be indicative of the cells' inability to repair damaged DNA; hence, we probed for damaged DNA with the comet assay. Figures 4A & B (graphical representation of data in 4A) show that exposure of SH-SY5Y cells to 2  $\mu\text{M}$  and 62  $\mu\text{M}$   $\text{Mn}^{2+}$  for 24 h resulted in an 8 and 9-fold increase in DNA damage compared to controls, respectively. Figure 4A shows the comet slide analysis of SH-SY5Y head and tail regions. Note the presence of comet tails at 2  $\mu\text{M}$  and 62  $\mu\text{M}$  Mn are not detected under control conditions. Figure 4B shows quantitative data of four replicates for each concentration,  $p < 0.05$ . This finding led us to hypothesize that reinforcing the cell's antioxidant defenses via exogenous supplementation of antioxidant molecules would provide protection from  $\text{Mn}^{2+}$ -induced DNA damage.

### 3.5 Glutathione and N-acetylcysteine protect SH-SY5Y cells from manganese-induced DNA single strand breaks

To test the hypothesis that exogenous antioxidants protect against  $\text{Mn}^{2+}$ -induced DNA damage, we supplemented the culture media with either 1 mM GSH or 1 mM NAC, 3h prior to a 24 h  $\text{Mn}^{2+}$  exposure (24 h time chosen based on results presented in Figure 4). The protective effects of GSH or NAC against  $\text{Mn}^{2+}$ -induced DNA damage to SH-SY5Y cells, assessed by comet assay analysis, are shown in Figure 5ABC. Significant decreases ( $p < 0.0001$ ) in comet tail length were observed in SH-SY5Y cells pretreated with either GSH or NAC prior to addition of Mn vs. SH-SY5Y treated with Mn alone (2  $\mu\text{M}$  or 62  $\mu\text{M}$ ). NAC and GSH each provided protection against Mn-induced formation and accumulation of DNA single strand breaks. Figure 5B and 5C (graphical representation of data in 5A) indicate that pre-treatment with GSH followed by 24 h exposure to 2  $\mu\text{M}$   $\text{Mn}^{2+}$  provided 84% (+/- 5%) protection and 58% (+/- 5%) protection at 62  $\mu\text{M}$  Mn; while pre-treatment with NAC followed by 24 h exposure to 62  $\mu\text{M}$   $\text{Mn}^{2+}$  provided 63% (+/- 5%) at 2  $\mu\text{M}$   $\text{Mn}^{2+}$  and 87% (+/- 5%) protection from DNA damage at 62  $\mu\text{M}$   $\text{Mn}^{2+}$ , respectively. The data shown are representative of three independent experiments each performed in triplicates. It should be noted that NAC or GSH alone had no effect on SH-SY5Y cell viability. That the observed DNA damage could be blocked by antioxidants, strongly suggests the involvement of

oxidative stress in the mechanism of Mn-induced DNA damage and apoptosis in SH-SY5Y cells.

### 3.6 Manganese-induced the formation and accumulation of oxidatively modified DNA base lesions in SH-SY5Y cells

In order to determine if Mn exposure results in the formation and accumulation of oxidatively modified DNA base damage, we utilized isotope dilution GC/MS to measure individual lesion levels. In our analysis, we were only able to detect background levels and changes in guanine-derived (8-OH-Gua, FapyGua) and thymine-derived (5-OH-5-MetHyd) lesions. We observed statistically significant accumulation of 5-OH-5-MetHyd at Mn doses of 62  $\mu\text{M}$  ( $p < 0.01$ ) and 125  $\mu\text{M}$  ( $p < 0.05$ ), but no statistically significant accumulations of either 8-OH-Gua nor FapyGua across the Mn exposure range (Figure 6A).

### 3.7 Glutathione and N-acetylcysteine protect SH-SY5Y cells from manganese-induced DNA base modifications

The observation that Mn (2  $\mu\text{M}$  and 62  $\mu\text{M}$ ) induced a statistically significant increase in the level of 5-OH-5MetHyd prompted us to test the hypothesis that exogenous antioxidants could protect against Mn-induced accumulation of modified thymine bases. We supplemented the culture media with either 1 mM GSH or 1 mM NAC 3 h prior to a 24 h Mn exposure. The protective effects of GSH or NAC are shown in Figures 6B & 6C, respectively. Significant decreases ( $p < 0.01$ ) in the formation and accumulation of 5-OH-5MetHyd were observed in SH-SY5Y cells pretreated with either NAC (Figure 6B) or GSH (Figure 6C) as compared to cells treated with Mn alone. Note, significant reduction by pretreatment with GSH on the accumulation of 5-OH-5MetHyd was not observed at the highest Mn concentration (125  $\mu\text{M}$ ).

## 4. Discussion

The purpose of the present study was to test the hypothesis that Mn<sup>2+</sup> induces apoptotic cell death through a series of events involving oxidatively damaged DNA using the SH-SY5Y neuronal-like cell line as a model. The human neuroblastoma SH-SY5Y cell line, a well-characterized neuronal-like model, extensively used for *in vitro* neurotoxicity testing, was chosen for this study because it could be induced to differentiate into the adrenergic phenotype (Pahlman et al. 1983). MnCl<sub>2</sub> was chosen because it is the divalent cation that is predominately found inside of cells (Roels et al. 1997), and because the chloride salt is water-soluble. This is the first study to sequentially investigate the effects of Mn<sup>2+</sup> on cytotoxicity, apoptosis, DNA damage, and protection from DNA damage by antioxidants. Our overall novel findings showed that Mn (2 $\mu\text{M}$  and 62 $\mu\text{M}$ ) caused a concentration-dependent decrease in cell viability after 24 h (Fig. 1A), DNA damage (strand breaks; Fig. 4) and induced oxidative lesions in thymine bases (termed 5-hydroxy-5-methylhydantoin; Fig. 6) in SH-SY5Y cells, a catecholaminergic cell model. NAC and GSH protected SH-SY5Y cells from Mn<sup>2+</sup>-induced DNA damage (Fig 5) strongly suggesting the involvement of ROS in these toxic processes. The beneficial effects of pre-treating with NAC and GSH are related to the ability of NAC to promote synthesis of endogenous GSH and the ability of GSH to scavenge and neutralize free radicals. Consistent with our results for SH-SY5Y neuronal-like cells are findings that GSH and NAC play major roles in modulating ROS in neuronal cells (Desole et al. 1997a; Desole et al. 1997b; Dukhande et al. 2006; Isaac et al. 2006; Marreilha dos Santos et al. 2008). Taken together, these novel findings support the hypothesis that oxidative DNA damage, specifically thymine lesions play a key role in mediating Mn<sup>2+</sup>-induced apoptotic cell death in SH-SY5Y cells.

The precise mechanisms that underlie Mn-induced neurodegeneration have yet to be fully understood. Multivalent metallic ions, such as Mn<sup>2+</sup> and Mn<sup>3+</sup>, readily react with biogenic amines (e.g., dopamine) through Fenton's reactions (redox cycling reactions) thus generating reactive radicals and/or reactive-oxygen species (ROS) and oxidative damage (Parenti et al, 1988; Donaldson et al 1981; Lloyd 1995; Donaldson et al, 1982; Shen et al, 1998; Ahmadi et al, 1998). Several mechanisms for Mn-catalyzed dopamine (DA) auto-oxidation have been proposed (Lloyd 1995; Shen et al, 1998; Donaldson et al, 1981; Ahmadi et al, 1998; Baranyi et al, 2006; Graumann, et al, 2002; Florence et al, 1989; Oikawa et al 2006). Consistent with these observations, our findings suggest that Mn catalyzed autooxidation of catecholamines in SH-SY5Y cells caused semiquinone radical ions or highly reactive oxidative species (ROS), ensuing in oxidative damage to thymine and guanine DNA bases (Fig 6A & 6B).

Exposure to Mn has been intimately associated with the neurodegenerative disorder, IPD. The primary cause of IPD is unknown, but thought to be due to exposure to environmental neurotoxicants (e.g. pesticides and Pb and Mn). Of these, Mn has been shown to be highly correlated with IPD given its propensity to accumulate in the same brain areas affected in IPD (Benedetto, 2009; Aschner, 2000). Furthermore, the strongest correlation between environmental exposure to a metal or pesticide and increased susceptibility to IPD has been uncovered in Mn-exposed populations (Gorell et al., 1999b) with occupational exposure to Mn for greater than 20 years being positively correlated with increased prevalence of IPD. Given our observations on Mn-induced thymine lesions as an important trigger in neurotoxicity, exploratory studies to further this hypothesis could be profitably directed at examining IPD patients' brain biopsies for DNA peroxidation products and thymine lesions.

## 5. Conclusion

We showed that low Mn<sup>2+</sup> caused oxidative damage to thymine DNA bases which could be attenuated by 1 mM NAC or 1 mM GSH. That the observed DNA damage could be lessened by antioxidants, strongly suggests the involvement of oxidative stress in the Mn<sup>2+</sup>-induced DNA damage and apoptosis in SH-SY5Y cells. We have not identified the source of ROS since the limits of detection of our Manganese peroxide assay was not in the range of the Mn<sup>2+</sup> concentrations that caused oxidative damage to the DNA bases in this study.

## Acknowledgments

The authors gratefully acknowledge the help of Alycia L. Buford for invaluable assistance in preparation of this manuscript; the technical assistance of Inneke Johnson, PhD and Latasha Fisher, MA. APS acknowledges graduate support from Florida McKnight Foundation and Florida A&M University School of Graduate Studies and Florida A&M University College of Pharmacy & Pharmaceutical Sciences.

We are appreciative of support from the following funding agencies: Association Of Minority Health Professions Schools, Inc (AMPHS) & the ATS/DR Cooperative Agreement Number: 3U50TS473408-05W1/CFDA Number 93.161 (RRR) NIEHS/ARCH 5S11ES01187-05 (RRR) and NIEHS R01 ES10653 (MA). Florida A&M University RCMI Grant # 2G12RR03020-25/NCRR/RCMI (KFAS)

## References

- Ahmadi FA, Grammatopoulos TN, Poczobutt AM, Jones SM, Snell LD, Das M, Zawada WM. Dopamine selectively sensitizes dopaminergic neurons to rotenone-induced apoptosis. *Neurochem Res.* 2008 May; 33(5):886–901. [PubMed: 17992568]
- Aisen P, Aasa R, Redfield AG. The chromium, manganese, and cobalt complexes of transferrin. *J Biol Chem.* 1969; 244:4628–4633. [PubMed: 4309148]
- Aschner M. Neuron-astrocyte interactions: implications for cellular energetics and antioxidant levels. *Neurotoxicology.* 2000 Dec; 21(6):1101–7. [PubMed: 11233756]

- Baly DL, Keen CL, Hurley LS. Pyruvate carboxylase and phosphoenolpyruvate carboxykinase activity in developing rats: effect of manganese deficiency. *J Nutr.* 1985; 115:872–879. [PubMed: 4009297]
- Baranyi M, Milusheva E, Vizi ES, Sperlagh B. Chromatographic analysis of dopamine metabolism in a Parkinsonian model. *J Chromatogr A.* 2006 Jul 7; 1120(1–2):13–20. [PubMed: 16580006]
- Benedetto A, Au C, Aschner M. Manganese-Induced Dopaminergic Neurodegeneration Insights Into Mechanism and Genetics Shared with Parkinson's Disease. *Chem Rev.* 2009; 109:4862–4884. [PubMed: 19534496]
- Biedler JL, Helson L, Spengler BA. Morphology and growth, tumorigenicity, and cytogenetics of human neuroblastoma cells in continuous culture. *Cancer Res.* 1973; 33:2643–2652. [PubMed: 4748425]
- Bowler RM, Roels HA, Nakagawa S, et al. Dose-effect relationships between manganese exposure and neurological, neuropsychological and pulmonary function in confined space bridge welders. *Occupational and Environmental Medicine.* 2007; 64:167–177. [PubMed: 17018581]
- Bowler RM, Gocheva V, Harris M, Ngo L, Abdelouahab N, Wilkinson J, Doty RL, Park R, Roels HA. Prospective study on neurotoxic effects in manganese-exposed bridge construction welders. *Neurotoxicology.* 2011; 32(5):596–605. [PubMed: 21762725]
- Brock CJ, Walker JE. Superoxide dismutase from *Bacillus stearothermophilus*. Complete amino acid sequence of a manganese enzyme. *Biochemistry.* 1980; 19:2873–2882. [PubMed: 7397109]
- Chen CJ, Liao SL. Oxidative stress involves in astrocytic alterations induced by manganese. *Exp Neurol.* 2002; 175:216–225. [PubMed: 12009774]
- Critchfield JW, Keen CL. Manganese + 2 exhibits dynamic binding to multiple ligands in human plasma. *Metabolism.* 1992; 41:1087–1092. [PubMed: 1406294]
- Desole MS, Esposito G, Migheli R, Sircana S, Delogu MR, Fresu L, Miele M, de Natale G, Miele E. Glutathione deficiency potentiates manganese toxicity in rat striatum and brainstem and in PC12 cells. *Pharmacol Res.* 1997a; 36:285–292. [PubMed: 9425617]
- Desole MS, Sciola L, Delogu MR, Sircana S, Migheli R, Miele E. Role of oxidative stress in the manganese and 1-methyl-4-(2'-ethylphenyl)-1,2,3,6-tetrahydropyridine-induced apoptosis in PC12 cells. *Neurochem Int.* 1997b; 31:169–176. [PubMed: 9220449]
- Dorman DC, Struve MF, Marshall MW, Parkinson CU, James RA, Wong BA. Tissue manganese concentrations in young male rhesus monkeys following subchronic manganese sulfate inhalation. *Toxicol Sci.* 2006; 92:201–210. [PubMed: 16624849]
- Donaldson J, LaBella FS, Gesser D. Enhanced autooxidation of dopamine as a possible basis of manganese neurotoxicity. *Neurotoxicology.* 1981 Jan; L2(1):53–64. [PubMed: 15622724]
- Donaldson J, McGregor D, LaBella F. Manganese neurotoxicity: a model for free radical mediated neurodegeneration? *Can J Physiol Pharmacol.* 1982 Nov; 60(11):1398–405. [PubMed: 6129921]
- Dukhande VV, Malthankar-Phatak GH, Hugus JJ, Daniels CK, Lai JC. Manganese-induced neurotoxicity is differentially enhanced by glutathione depletion in astrocytoma and neuroblastoma cells. *Neurochem Res.* 2006; 31:1349–1357. [PubMed: 17053969]
- Falcieri E, Martelli AM, Bareggi R, Cataldi A, Cocco L. The protein kinase inhibitor staurosporine induces morphological changes typical of apoptosis in MOLT-4 cells without concomitant DNA fragmentation. *Biochem Biophys Res Commun.* 1993; 193:19–25. [PubMed: 8503906]
- Florence TM, Stauber JL. Manganese catalysis of dopamine oxidation. *Sci Total Environ.* 1989 Jan; 78:233–40. [PubMed: 2541499]
- Gorell JM, Johnson CC, Rybicki BA, Peterson EL, Kortsha GX, Brown GG, Richardson RJ. Occupational exposure to manganese, copper, lead, iron, mercury and zinc and the risk of Parkinson's disease. *Neurotoxicology.* 1999a; 20:239–247. [PubMed: 10385887]
- Gorell JM, Rybicki BA, Cole Johnson C, Peterson EL. Occupational metal exposures and the risk of Parkinson's disease. *Neuroepidemiology.* 1999b; 18:303–308. [PubMed: 10545782]
- Graumann R, Paris I, Martinez-Alvarado P, Rumanque P, Perez-Pastene C, Cardenas SP, Marin P, Diaz-Grez F, Caviedes R, Caviedes P, Segura-Aguilar J. Oxidation of dopamine to aminochrome as a mechanism for neurodegeneration of dopaminergic systems in Parkinson's disease. Possible neuroprotective role of DT-diaphorase. *Pol J Pharmacol.* 2002 Nov-Dec; L54(6):573–9. [PubMed: 12866711]

- Isaac AO, Kawikova I, Bothwell AL, Daniels CK, Lai JC. Manganese treatment modulates the expression of peroxisome proliferator-activated receptors in astrocytoma and neuroblastoma cells. *Neurochem Res.* 2006; 31:1305–1316. [PubMed: 17053972]
- Jalava A, Heikkila J, Lintunen M, Akerman K, Pahlman S. Staurosporine induces a neuronal phenotype in SH-SY5Y human neuroblastoma cells that resembles that induced by the phorbol ester 12-O-tetradecanoyl phorbol-13 acetate (TPA). *FEBS Lett.* 1992; 300:114–118. [PubMed: 1348695]
- Kim Y, Kim JW, Ito K, Lim HS, Cheong HK, Kim JY, Shin YC, Kim KS, Moon Y. Idiopathic parkinsonism with superimposed manganese exposure: utility of positron emission tomography. *Neurotoxicology.* 1999; 20:249–252. [PubMed: 10385888]
- Lloyd RV. Mechanism of the Manganese-catalyzed autoxidation of Dopamine. *Chem Res Toxicol.* 1995 Jan-Feb;8(1):111–6. [PubMed: 7703354]
- Marreilha dos Santos AP, Santos D, Au C, Milatovic D, Aschner M, Batoreu MC. Antioxidants prevent the cytotoxicity of manganese in RBE4 cells. *Brain Res.* 2008; 1236:200–205. [PubMed: 18725210]
- Normandin L, Panisset M, Zayed J. Manganese neurotoxicity: behavioral, pathological, and biochemical effects following various routes of exposure. *Rev Environ Health.* 2002; 17:189–217. [PubMed: 12462483]
- Oikawa S, Hirose I, Tada-Oikawa S, Furukawa A, Nishiura K, Kawanishi S. Mechanism for manganese enhancement of dopamine-induced oxidative DNA damage and neuronal cell death. *Free Radic Biol Med.* 2006 Sep 1; 41(5):748–56. [PubMed: 16895795]
- Pahlman S, Odelstad L, Larsson E, Grotte G, Nilsson K. Phenotypic changes of human neuroblastoma cells in culture induced by 12-O-tetradecanoyl-phorbol-13-acetate. *Int J Cancer.* 1981; 28:583–589. [PubMed: 7309295]
- Pahlman S, Ruusala AI, Abrahamsson L, Odelstad L, Nilsson K. Kinetics and concentration effects of TPA-induced differentiation of cultured human neuroblastoma cells. *Cell Differ.* 1983 Mar; 12(3):165–70. [PubMed: 6299586]
- Parenti M, Rusconi L, Cappabianca V, Parati EA, Groppetti A. Role of dopamine in manganese neurotoxicity. *Brain Res.* 1988 Nov 15; 473(2):236–40. [PubMed: 2852985]
- Racette BA, McGee-Minnich L, Moerlein SM, Mink JW, Videen TO, Perlmutter JS. Welding-related parkinsonism: clinical features, treatment, and pathophysiology. *Neurology.* 2001; 56:8–13. [PubMed: 11148228]
- Reddy P, Jaruga P, O'Connor T, Rodriguez H, Dizdaroglu M. Overexpression and rapid purification of Escherichia coli formamidopyrimidine-DNA glycosylase. *Protein Expr Purif.* 2004; 34:126–33. [PubMed: 14766308]
- Roels H, Meiers G, Delos M, Ortega I, Lauwerys R, Buchet JP, Lison D. Influence of the route of administration and the chemical form (MnCl<sub>2</sub>, Mn O<sub>2</sub>) on the absorption and cerebral distribution of manganese in rats. *Arch Toxicol.* 1997; 71(4):223–30. [PubMed: 9101038]
- Seth K, Agrawal AK, Date I, Seth PK. The role of dopamine in manganese-induced oxidative injury in rat pheochromocytoma cells. *Hum Exp Toxicol.* 2002; 21:165–170. [PubMed: 12102543]
- Shen XM, Dryhurst G. Iron and manganese-catalyzed autoxidation of dopamine in the presence of L-cysteine possible insights into iron- and manganese-mediated dopaminergic neurotoxicity. *Chem Res Toxicol.* 1998 Jul; 11(7):824–37. [PubMed: 9671546]
- Singh NP, Mc Coy MT, Tice RR, Schneider EL. A simple technique for quantitation of low levels of DNA damage in individual cells. *Exp Cell Res.* 1988 Mar; 175(1):184–91. [PubMed: 3345800]
- Stredrick DL, Stokes AH, Worst TJ, Freeman WM, Johnson EA, Lash LH, Aschner M, Vrana KE. Manganese-induced cytotoxicity in dopamine-producing cells. *Neurotoxicology.* 2004; 25:543–553. [PubMed: 15183009]
- Takeda Y, Avila H. Structure and gene expression of the E. coli Mn-superoxide dismutase gene. *Nucleic Acids Res.* 1986; 14:4577–4589. [PubMed: 3520487]
- Wang CY, Jenkitkasemwong S, Duarte S, Sparkman BK, Shawki A, Mackenzie B, Knutson MD. ZIP8 is an iron and zinc transporter whose cell-surface expression is up-regulated by cellular iron loading. *J Biol Chem.* 2012 Oct 5; 287(41):34032–43. Epub 2012 Aug 16. 10.1074/jbc.M112.367284 [PubMed: 22898811]

- Weber S, Dorman DC, Lash LH, Erikson K, Vrana KE, Aschner M. Effects of manganese (Mn) on the developing rat brain: oxidative-stress related endpoints. *Neurotoxicology*. 2002; 23:169–175. [PubMed: 12224758]
- Worley CG, Bombick D, Allen JW, Suber RL, Aschner M. Effects of manganese on oxidative stress in CATH.a cells. *Neurotoxicology*. 2002; 23:159–164. [PubMed: 12224756]

### Highlights

Manganese chloride promotes oxidative DNA damage in cultured SH-SY5Y neuronal cells.

The accumulated DNA damage resulted in cell death via an apoptotic pathway.

DNA strand breaks/thymine lesions were measured by comet and mass spec analysis.

The oxidative DNA damage may be associated with Mn-induced reactive oxygen species.

The addition of exogenous antioxidants can reduce the accumulated DNA damage.

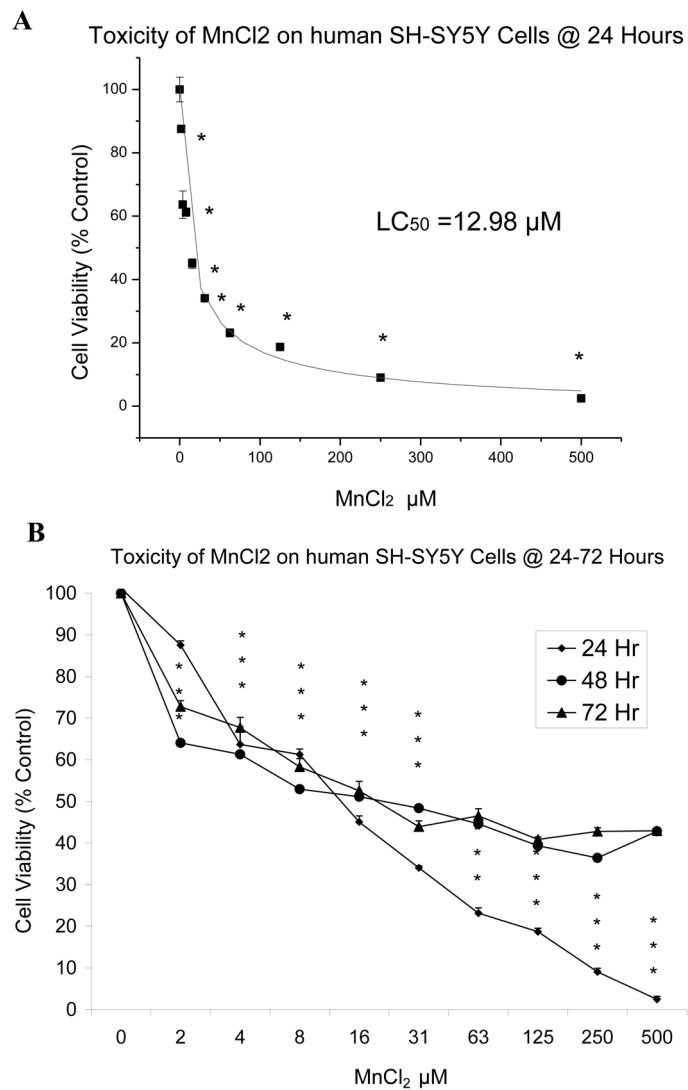


**Figure 1.** Effect of MnCl<sub>2</sub> on cell viability in SH-SY5Y cells. SH-SY5Y cells were exposed to Mn (0 μM to 500 μM) for 24 h (A), 48 and 72 h (A & B) as described. Cell viability was determined by Almar Blue assay, cell viability is displayed as the mean ± SD, n=8, and statistically significant data determined by a one-way ANOVA, with Dunn's post hoc test (\*p < 0.001 vs. control).

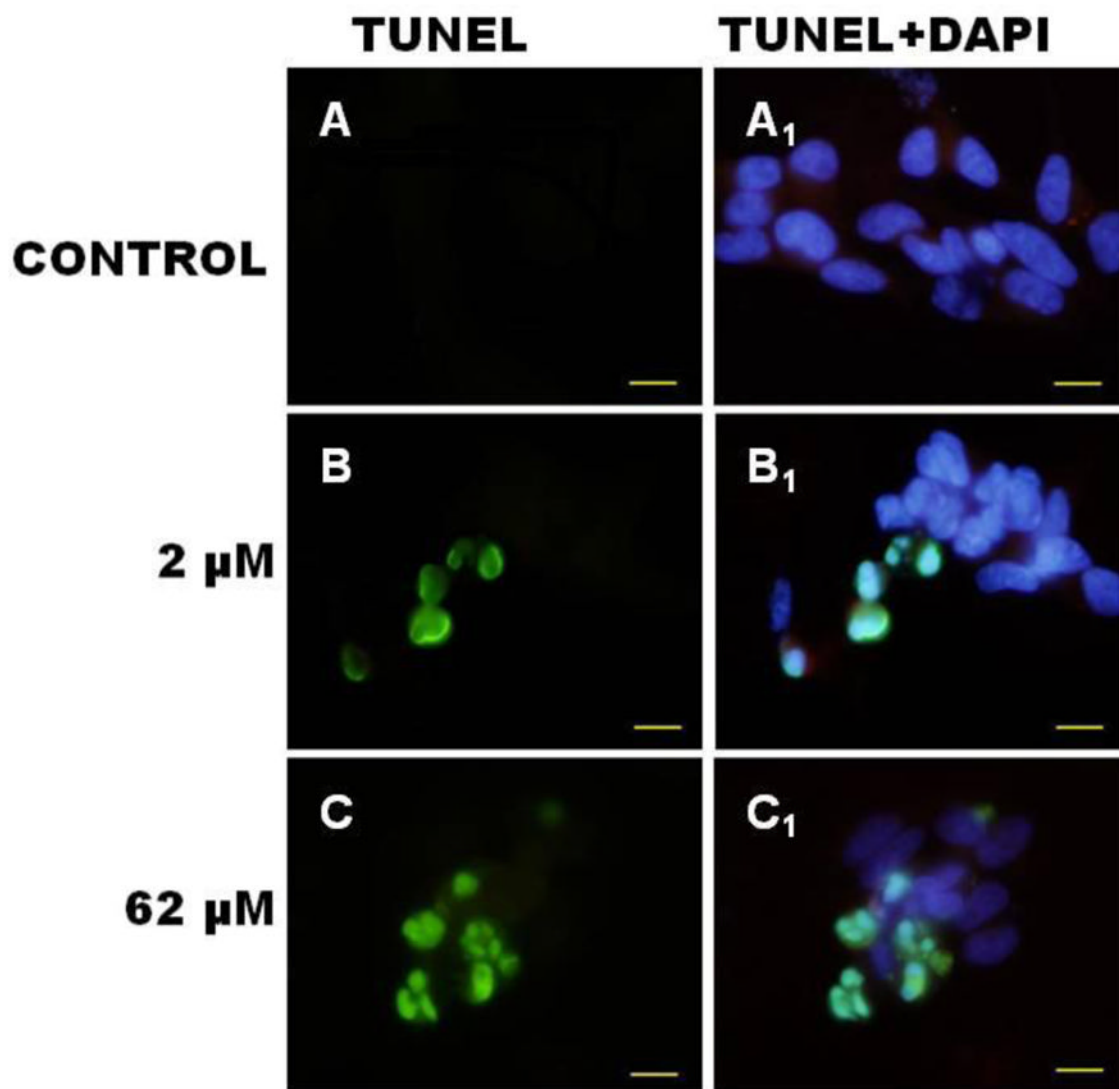


**Figure 2.** Photomicrograph of neuronal SH-SY5Y cells stained with TUNEL and DAPI following 24 h exposure to Mn. Top panel represents control (untreated cells); middle panel represents 24 h exposure to 2 μM Mn<sup>2+</sup>. Bottom panel: represents 24 h exposure to 62 μM Mn<sup>2+</sup>. DNA fragmentation is indicated by TUNEL-positive staining (green) in frames A–C. Nuclear condensation and clumping indicated by DAPI nuclear staining (blue) in frames A<sub>1</sub>–C<sub>1</sub> is co-localized in degenerating cells at 24 h. Micron bar represent 10 μm (micrometers).

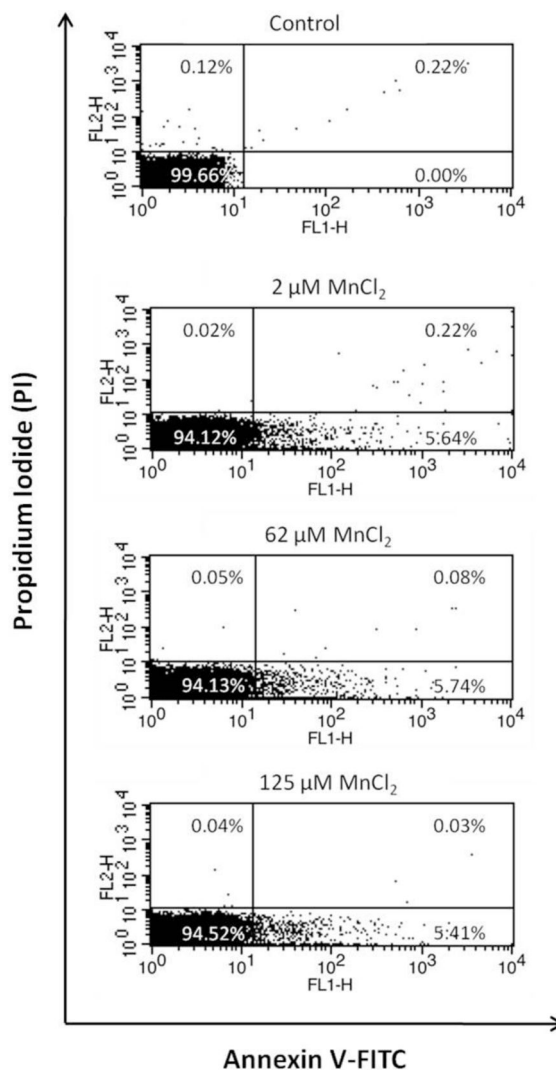


**Figure 3.** Apoptosis of SH-SY5Y cells treated with different Mn concentrations was assessed using annexin V/PI staining and flow cytometry. Quadrants: lower left: live cells; lower right: early apoptotic cells; upper right: late apoptotic cells and upper left: necrotic cells. Pearson's correlation test and paired t-test were used for statistical analysis of data from triplicate independent flow cytometry experiments.

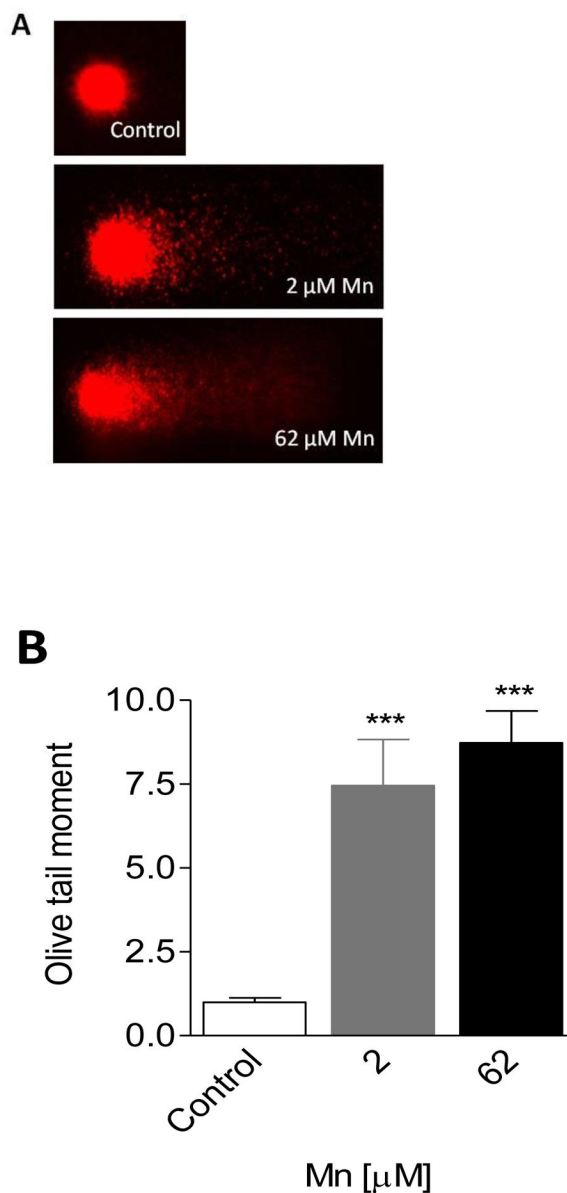


**Figure 4. Comet assay determination of single strand breaks (SSBs) in SH-SY5Y cells after exposure to Mn**

Panel A: Representative photomicrographs of Mn-induced DNA damage in SH-SY5Y cells using comet assay. Neuronal like SH-SY5Y cells were treated with Mn<sup>2+</sup> (2 μM or 62 μM) for 24 h. Controls were not treated with Mn<sup>2+</sup>.

Panel B: Mean olive tail moment was calculated for each treatment and control. Data plotted represents differences in DNA damage between control and treatments. Controls provide an estimate of background DNA strand breaks (SB) in the absence of Mn<sup>2+</sup>. Results are significant difference (\*\*\*)  $p < .0001$ ) between neuronal SH-SY5Y control and Mn<sup>2+</sup> treated cells by one-way ANOVA.

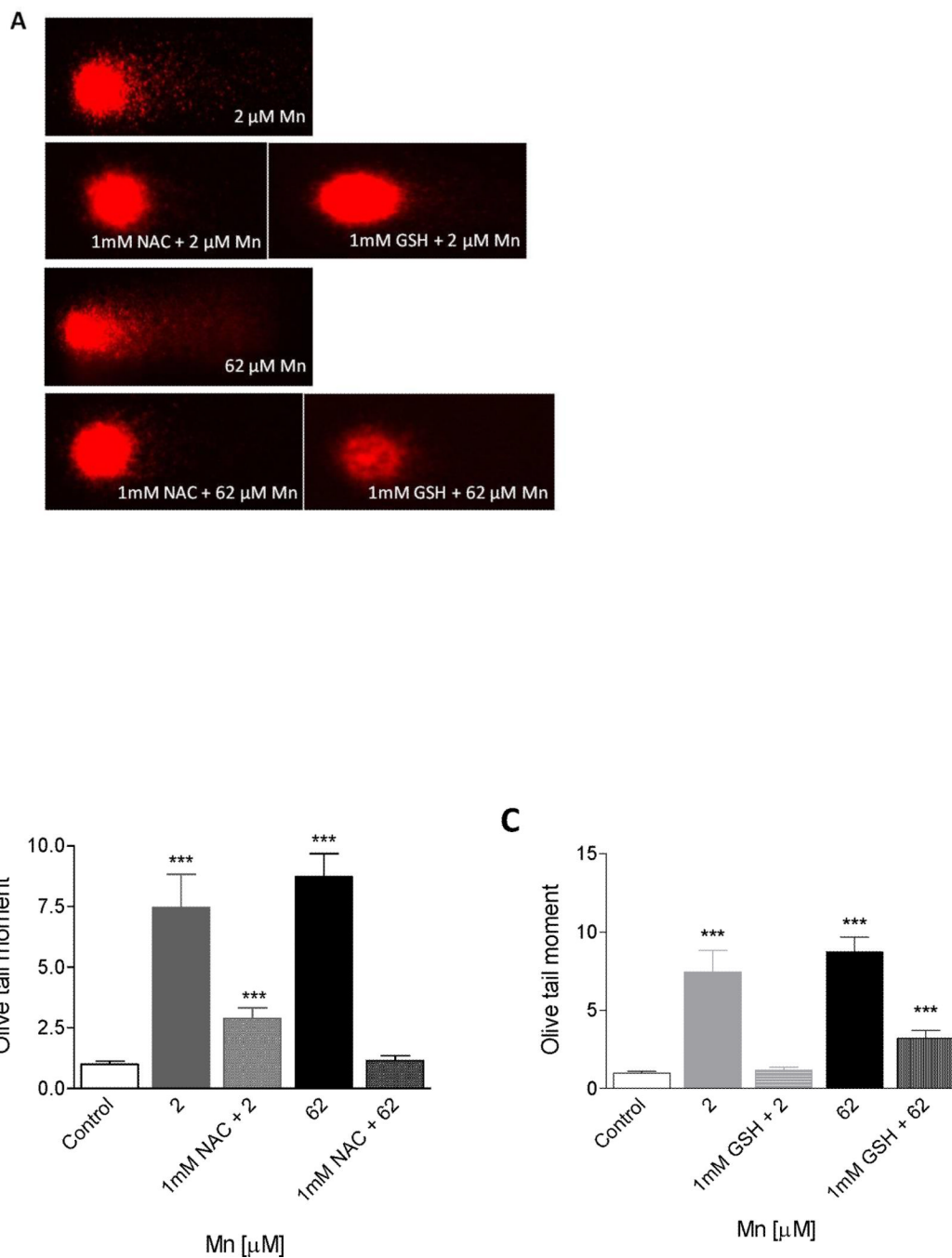


**Figure 5. Comet assay analysis of single strand breaks in SH-SY5Y cells after exposure to Mn<sup>2+</sup>: effect of exogenous antioxidants**

Panel A: DNA damage in neuronal SH-SY5Y cells following pretreatment with NAC or GSH then 24 h exposure to Mn<sup>2+</sup> using the comet assay. SH-SY5Y cells were pretreated with 1 mM NAC or 1 mM GSH for 3 h followed by 24 h exposure to Mn<sup>2+</sup> (2  $\mu$ M and 62  $\mu$ M).

Panels B,C: Mean olive tail moment was calculated for each treatment and control. Data plotted represents differences in DNA damage between control and treatments. Controls provide an estimate of the background of DNA strand breaks (SB) in the absence of Mn.

Results are significant difference (\*\* $p < .0001$ ) between neuronal SH-SY5Y control and Mn<sup>2+</sup> treated cells by one-way ANOVA.)

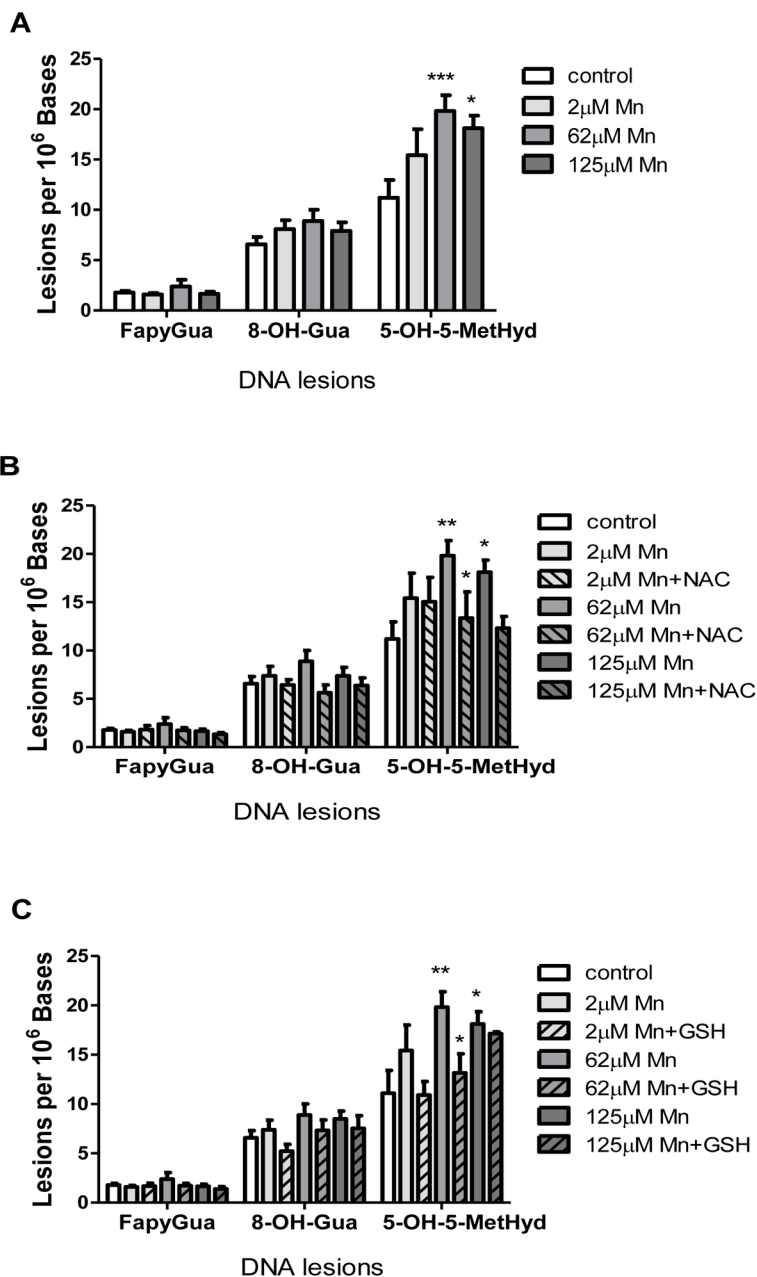


**Figure 6. Mn<sup>2+</sup>-induced DNA base lesions in SH-SY5Y cells**

Panel A: Levels of FapyGua, 8-OH-Gua, and 5-OH-5-MetHyd lesions in DNA isolated from SH-SY5Y cells following 24 h exposure to Mn<sup>2+</sup> were quantified using GC/MS.

Experiments were conducted as described in Materials and Methods. Values represent mean  $\pm$  SD of three independent experiments. Two-way analysis of variance with the Bonferroni post test was used to evaluate significance relative to the control and is denoted by (\*). 5-OH-5-MetHyd: \*P < 0.05, \*\*P < 0.01.

Panel B: Protective effect of NAC on Mn<sup>2+</sup>-induced DNA lesions in SH-SY5Y cells.

Quantification of FapyGua, 8-OH-Gua, and 5-OH-5-MetHyd DNA base lesions isolated from SH-SY5Y pre-treated with NAC, followed by Mn<sup>2+</sup> dosing as described in Materials and Methods. Values represent mean  $\pm$  SD of three independent experiments. Two-way

analysis of variance with the Bonferroni post test was used to evaluate significance relative to the control and is denoted by (\*). 5-OH-5-MetHyd: \*P < 0.05, \*\*P < 0.01.

Panel C: Protective effect of GSH on Mn<sup>2+</sup>-induced DNA base lesions in SH-SY5Y cells. Quantification of FapyGua, 8-OH-Gua, and 5-OH-5-MetHyd DNA base lesions isolated from SH-SY5Y pre-treated with GSH, followed by Mn<sup>2+</sup> dosing as described in Materials and Methods. Values represent mean ± SD of three independent experiments. Two-way analysis of variance with the Bonferroni posttest was used to evaluate significance relative to the control and is denoted by (\*). 5-OH-5-MetHyd: \*P < 0.05, \*\*P < 0.01.